Supporting Information: Mode Coarsening or Fracture: Energy Transfer Mechanisms in Rods Dynamic Buckling

E. Villermaux[1,2,3], K. Keremidis[4], N. Vandenberghe[2], M.J. Abdolhosseini Qomi[5] and F.-J. Ulm[1,4,*]
[1] *MIT-CNRS Joint Lab 'Multiscale Materials Science for Energy and the Environment'. Massachusetts Institute of Technology. Cambridge 02139, USA.*
[2] *Aix Marseille Université CNRS Centrale Marseille IRPHE Marseille, France.*
[3] *Institut Universitaire de France.*
[4] *Department of Civil and Environmental Engineering. Massachusetts Institute of Technology. Cambridge MA 02139, USA.*
[5] *Department of Civil and Environmental Engineering. University of California Irvine. Irvine California 92697 USA.*

In this Supporting Information, we provide (1) details about the experimental setup and the repeatability of the experiments; (2) the derivation of the force relaxation relation during dynamic postbuckling; (3) the post-buckling solutions with a transient force relaxation; and (4) additional information about the MD-inspired structural simulations.

PACS numbers: find pacs

EXPERIMENTAL SETUP AND REPEATABILITY

The experimental setup is illustrated in Fig. 1 by one out of the many impact tests we made. The wood beam, clamped at one side, is impacted longitudinally by a heavy (much heavier than the beam itself so that the transfer of inertia is made at constant velocity) steel cylinder falling by its own weight. The beam extremity on the impactor side is guided and the impact results in an effective shortening of the available distance between the extremities of the beam. While the direction of the beam deflection is initially random from one test to the other, the distortions wavelengths of the beam, and progressive coarsening are deterministic, perfectly repeatable from one test to the other. The same setup, and observations, apply when the beam is made of dry, brittle pasta.

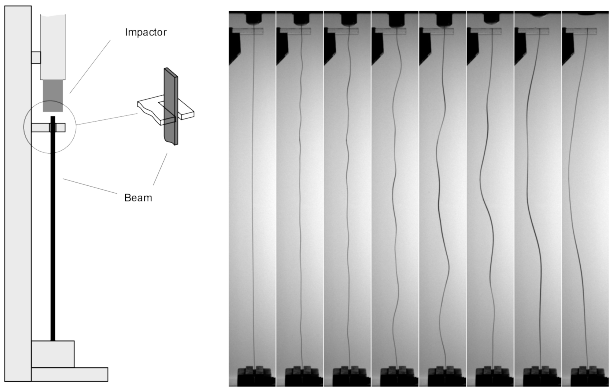

FIG. 1: Sketch of the experimental setup and sequence of images of the distorted beam after impact. The 720 cm long beam, made of hard wood, is clamped at one extremity and allowed to slide during impact at the other extremity, after what it remains clamped. The sequence of images (snapshot taken at t= 0 ; 0.5 ms ; 1 ms ; 2.5 ms ; 7.5 ms ; 12.5 ms ; 25 ms ; 50 ms) reveals the development of the short wavelength buckling at short times, and the subsequent coarsening dynamics.

GEOMETRIC FORCE RELAXATION MODEL

Consider the beam bending differential equation for lateral deflection, $\xi(x,t)$, of a beam (length ℓ, cross section A, moment of geometric inertia $I = Ad^2$, geometric radius of gyration $d = \sqrt{I/A}$, mass density ρ, Young's modulus E), subject to a compressive force P:

$$\rho A\ddot{\xi} + \frac{\partial^2}{\partial x^2}\left(EI\xi''\right) + \frac{\partial}{\partial x}\left(P\xi'\right) = 0 \qquad (1)$$

with overdot denoting time derivative, and prime derivative along the rod's axis x. The force P is generated by an impact of a projectile (project velocity U_0) hitting one end of the rod, and propagating at the speed of sound, $c = \sqrt{E/\rho}$, along the rod's axis to the other end. Considering $\xi \sim \exp(ikx - i\omega t)$, we readily find that force P will entail an instability ($\omega \to 0$) associated with a wavenumber $k_c = k(\omega \to 0) = \sqrt{P/EI}$. Hence, as the force decreases, it is recognized that the buckling shifts from higher wavenumbers to lower wavenumbers. This motivates the development of a first-order geometric force relaxation mechanism model.

Consider thus an instability of the form $\xi(x) \sim \xi_k \sin(kx)$ along $x \in [0, \ell - \delta\ell]$, with ξ_k some magnitude, and $\delta\ell$ the shortening induced by the impact of the projectile. If the force P was zero, length preservation requires:

$$\begin{aligned} \ell &= \int_0^{\ell-\delta\ell} \sqrt{1+\xi'^2}dx \approx \int_0^{\ell-\delta\ell}\left(1+\frac{1}{2}\xi'^2\right)dx \qquad (2)\\ &= (\ell-\delta\ell)\left(1+(\xi_k k)^2\right) \end{aligned}$$

We thus assume that such a relation equally holds when the force is non zero producing an axial shortening of the

rods length,$-\epsilon\ell = P(k)\,\ell/EA$, in the form $\ell(1-\epsilon) = (\ell-\delta\ell)\left(1+(\xi_k k)^2\right)$. This consideration readily provides a link between the residual force, $P(k)$, and the wavenumber, k, in the form:

$$\frac{P(k)}{EA} = \frac{\delta\ell}{\ell} - (\xi_k k)^2\left(1-\frac{\delta\ell}{\ell}\right) \approx \frac{P_0}{EA}\left(1-\frac{(\xi_k k)^2}{\delta\ell/\ell}\right) \tag{3}$$

where $P_0 = EA\ \delta\ell/\ell$ is the initial buckling force [1].

The beam deflection slope $\xi_k k \sim \sqrt{\delta\ell/\ell}$, varies between $\xi_k k \to 0$ and $(\xi_k k)^2 \to \delta\ell/\ell$ for a complete force relaxation (i.e. $P(k) \to 0$). Otherwise said, in the post-buckling regime, the force relaxation mechanism involves, from pure geometry, the increase in time of the instability magnitude ξ_k; The initial growth is such that $\xi_k(k) \sim \xi_0 t_k/\tau$ where τ is the buckling instability timescale $\tau \sim d/U_0$ [1]. Time t_k thus represents the time at which mode k determines the force $P(k)$:

$$t_k \sim \tau\frac{\sqrt{\delta\ell/\ell}}{\xi_0 k} \tag{4}$$

Incorporating this $t_k \sim k^{-1}$ relation in a continuous fashion into expression (3) yields the transient force relaxation relation:

$$P(t) = P_0\left(1-\left(\frac{t}{t_k}\right)^2\right) \geq 0 \tag{5}$$

That is, for $t < t_k$ a force relaxation takes place; whereas for $t > t(k)$, we have $P(t) = 0$.

POST-BUCKLING SOLUTIONS WITH A TRANSIENT FORCE RELAXATION

We are interested in solutions of the lateral deflection Eq. (1) considering the transient force expression (5). Spatial solutions we herein consider are of the form $\xi(x,t) = \xi_k(t)\exp(ikx)$; so that Eq. (1) is rewritten in the form:

$$\ddot{\xi}_k(t) + \omega_k^2\xi_k(t) = \frac{F}{t_k}, \quad \text{with} \quad F = k\frac{d}{\sqrt{U_0 c}}\frac{P(t)}{\rho A}\frac{\xi_k(t)}{\xi_0} \tag{6}$$

where $\omega_k = d\,c\,k^2$; and where we considered $\delta\ell/\ell = U_0/c$.

We first inspect Eq. (6) for $t < t_k$, for which $P(t) \simeq P_0 = EA\ U_0/c$, and $F \simeq F_0 = kd\sqrt{U_0 c}$. Considering solutions of the form $\xi_k = a_0 + a_1\cos\omega_k t + a_2\sin\omega_k t$, with initial conditions, $\xi_k(0) = \xi_0 = a_0 + a_1$, and $\dot{\xi}_k(0) = \omega_k a_2 = 0$, we readily find $\omega_k^2 a_0 = F_0/t_k$. Consider next $t > t_k$, for which $P(t) = 0$; and hence $F = 0$. Solutions of $\ddot{\xi}_k(t) + \omega_k^2\xi_k(t) = 0$ are of the form $\xi_k = b_1\cos\omega_k t + b_2\sin\omega_k t$. Finally, at $t = t_k$, we ensure continuity of ξ_k and $\dot{\xi}_k$, thus:

$$a_0 + a_1\cos\omega_k t_k = b_1\cos\omega_k t_k + b_2\sin\omega_k t_k \tag{7a}$$

$$-a_1\omega_k\sin\omega_k t_k = -b_1\omega_k\sin\omega_k t_k + b_2\omega_k\cos\omega_k t_k \tag{7b}$$

We consider solutions of this linear system of first order in t_k, which is obtained by a Taylor expansion w.r.t. $\omega_k t_k$. This yields $b_1 = \xi_0 + O\left((\omega_k t_k)^2\right)$ and $b_2 = F_0/\omega_k + O\left((\omega_k t_k)^3\right)$. Whence the final solution:

$$\xi_k(t) = \xi_0\cos(\omega_k t) + \frac{F_0}{\omega_k}\sin(\omega_k t) \tag{8}$$

Or equivalently,

$$\xi_k(t) = \xi_0\cos\left(dck^2 t\right) + \frac{\sqrt{U_0/c}}{k}\sin\left(dck^2 t\right) \tag{9}$$

Last, we are interested in a relation between the most amplified wavenumber k and time t when the maximum amplitude is reached; that is:

$$\frac{\partial\xi_k}{\partial k} = cdt\left(\sqrt{\frac{U_0}{c}} - 2ck^3 d\ t\xi_0\right) + O\left(k^4\right) = 0 \tag{10}$$

It follows the sought relation:

$$k = \left(\frac{\sqrt{U_0/c}}{2cd\ t\xi_0}\right)^{1/3} \tag{11}$$

Thus, as t increases the wavenumber k at which ξ_k reaches a maximum decreases, which justifies a posteriori the Taylor development in Eq. (10). Expression (11) thus captures the mode coarsening during the post-buckling phase. Note that this mode coarsening law is solely constrained by the inverse relation, $t_k \sim k^{-1}$ defined by Eq. (4), which enters the geometric force relaxation model (5).

MOLECULAR DYNAMICS (MD) INSPIRED BUCKLING SIMULATIONS

In contrast to earlier approaches which employed molecular chain models within the framework of Rouse dynamics to study the dynamics of Euler buckling instability [2], the MD-inspired molecular dynamics approach herein employed solves the equations of motions within the classical framework of MD-based simulations in either the micro-canonical ensemble (NVE) or the canonical ensemble (NVT). That is, simulations are based on a discretization of a structure in discrete mass points (here, 932 for wood ($l_{ij} = 1/931\,\ell = 0.773$ mm), and 564 for pasta ($l_{ij} = 1/563\,\ell = 0.444$ mm)); the description of interactions by means of potentials of mean force (PMFs) suitable for structural members for both two-body (stretch) and three-body (bending) interactions [3]; and –for NVT simulations– a thermalization using the Nosé–Hoover thermostat. The consideration of different thermodynamic ensembles is essential to appreciate the difference between the first-order analytical model derived above and the experimental observation of mode coarsening [see Fig. 3a in main text]. Furthermore, the classical MD/PMF-based framework permits fracture simulations. Details are provided below.

Harmonic Potentials

For the application to buckling problems, we consider –akin to earlier approaches [2]– harmonic potentials for both two-body,

$$U_{ij} = \frac{1}{2}\epsilon^n_{ij}\lambda^2_{ij} \tag{12}$$

and three-body interactions,

$$U_{ijk} = \frac{1}{2}\overrightarrow{\vartheta}^{jk}_i \cdot C_{ijk} \cdot \overrightarrow{\vartheta}^{jk}_i \tag{13}$$

where:

- ϵ^n_{ij} is the elastic energy parameter activated by two body interactions due to the stretch $\lambda_{ij} = (1/l_{ij})\left(\overrightarrow{r}_{ij} - \overrightarrow{r}^0_{ij}\right)\cdot\overrightarrow{n}^{ij}$ in direction $\overrightarrow{n}^{ij} = \overrightarrow{r}_{ij}/l_{ij}$ of the link between mass points i and j of length $l_{ij} = ||\overrightarrow{r}_{ij}||$. For beam time structures, it is readily recognized that $\epsilon^n_{ij}/l_{ij} = EA$ (with E the Young's modulus, A the beam's cross-section).

- C_{ijk} is the second-order tensor of rotational stiffness activayed by angular variations $\overrightarrow{\vartheta}^{jk}_i$:

$$\overrightarrow{\vartheta}^{jk}_i \simeq \frac{\overrightarrow{r}_{ij}\times\overrightarrow{r}^0_{ik} - \overrightarrow{r}^0_{ij}\times\overrightarrow{r}^0_{ik}}{||\overrightarrow{r}^0_{ij}||\ ||\overrightarrow{r}^0_{ik}||} \tag{14}$$

  For an initially straight beam with infinite torisonal rigidity, C_{ijk} is defined in the local coordinate system of the three-body link system $(\overrightarrow{n}^{ij}, \overrightarrow{b}^{ij}, \overrightarrow{t}^{ij})$ by:

$$C^{-1}_{ijk} = \left(\frac{\overrightarrow{t}^{ij}\otimes\overrightarrow{t}^{ij}}{\epsilon^b_{ij}} + \frac{\overrightarrow{b}^{ij}\otimes\overrightarrow{b}^{ij}}{\epsilon^t_{ij}}\right) \tag{15}$$

  where $\left(\epsilon^b_{ij}, \epsilon^t_{ij}\right)$ are bending energies which are readily available from a comparison with classical beam theory, namely $\epsilon^b_{ij} = EI_{bb}/l_{ij}$ and $\epsilon^t_{ij} = EI_{tt}/l_{ij}$; with I_{bb}, I_{tt} the second-order (bending) moments of geometric inertia $I_{bb} = \int_A x_b^2\ da$; $I_{tt} = \int_A x_t^2\ da$ $(da = dx_b dx_t)$.

In the simulations, we consider $E = 2.9$ GPa for pasta, and $E = 10$ GPa for wood, and determine the section parameter from the geometric dimensions of the rods, namely, for the dry paste of circular cross section of diameter $d = 8$ mm (see main text), $A = \pi d^2/4, I_{bb} = I_{tt} = \frac{1}{32}\pi d^4$; and for the reactangular wood section of width $b = 3.1$ mm and height $h = 0.53$ mm; $A = bd, I_{bb} = \frac{1}{12}hb^3$ and $I_{tt} = \frac{1}{12}bh^3$. Buckling deformation, $\xi(x,t)$, naturally, occurs around the weaker intertia axis, i.e. in the $\overrightarrow{t}^0-$ direction.

Cut-Off values

For fracture simulations, we consider a threshold value for the maximum admissible stretch and curvature variations. Consistent with fracture processes, these threshold values relate to the ground state energy, ϵ_0; that is (for a derivation, see [3]):

$$\lambda_{ij} \le \lambda_c = \left(\frac{2\epsilon_0}{\epsilon^n_{ij}}\right)^{1/2} \sim l_{ij}^{-1/2} \tag{16}$$

and

$$\frac{||\overrightarrow{\vartheta}^{jk}_i||}{l_{ij}} \le \frac{\vartheta_c}{l_{ij}} = \frac{\lambda_c}{\sqrt{d_b^2 + d_t^2}} = \frac{1}{l_{ij}}\left(\frac{2\epsilon_0}{\epsilon^b_{ij} + \epsilon^t_{ij}}\right)^{1/2} \sim l_{ij}^{-1/2} \tag{17}$$

where $d_b = \sqrt{I_{bb}/A}$ and $d_t = \sqrt{I_{tt}/A}$ stand for the section radii of gyration. In the dynamic fracture simulations of the pasta rod, we calibrated the value of the ground state energy to be $\epsilon_0 = 0.2$ J, which corresponds –at the chosen discretization level $(l_{ij}/\ell = 1/563)$– to a limit stretch of $\lambda_c = 0.078\,61$ and a limit angle of $\vartheta_c = 0.5°$. For other discretization levels, the scaling of the cut-off values with the square root of the bond length $l_{ij} \to l^0_{ij}$ ensures that such changes do (almost) not affect the formation of fracture patterns, while respecting the classical scaling of Linear Elastic Fracture Mechanics (for a discussion, see e.g. [4]).

Research carried out by the Concrete Sustainability Hub (CSHub@MIT), with funding provided by the Portland Cement Association (PCA) and the Ready Mixed Concrete Research & Education Foundation (RMC E&F). Additional support was provided by the joint MIT-CNRS research unit enabling the sabbatical of EV at MIT; and by NSF award 1826122 for MJAQ. All simulations were carried out with the open source code LAMMPS, distributed by Sandia National Laboratories, a US Department of Energy laboratory [5].

[1] J.R. Gladden, N.Z. Handzy, A. Belmonte, E. Villermaux, *Phys. Rev. Letters.* **94**, 035503 (2005).
[2] L. Golubovic, D. Moldovan, A. Peredera *Phys. Rev. Letters* **81** 3387 (1998).
[3] K Keremides, MJ Abdolhosseini Qomi, RJM Pellenq, F-J Ulm, *Journal of Engineering Mechanics* **144**(8), 04018066 (2018).
[4] Laubie, H., F. Radjai, R. Pellenq, and F.-J. Ulm, *J. Mech. Phys. Solids* **105**(8), 116–130 (2017).
[5] S. Plimpton, *J. Comput. Phys.* **117** (1): 1–19 (1995). https://doi.org/10.1006/jcph.1995.1039